MINIMIZING TOTAL RADIATION FLUENCE DURING TIME-CONSTRAINED ELECTRIC ORBIT-RAISING

Atri Dutta[(1)], Paola Libraro[(2)], Jeremy Kasdin[(3)], and Edgar Choueiri[(4)]
[(1)(2)(3)(4)]*Mechanical and Aerospace Engineering, Princeton University, Engineering Quadrangle, Princeton NJ 08544, {atrid, plibraro, jkasdin, choueiri}@princeton.edu*

Abstract: *Incident radiation within the Van Allen belt causes significant degradation of the solar arrays of a satellite and a major challenge is to reduce the total radiation exposure of the satellites during the orbit-raising maneuver. In this paper, we consider the problem of time-constrained electric orbit-raising problem that seeks to minimize the total radiation fluence incurred by a satellite during its transit through the Van Allen belts. We use a direct optimization based methodology and incorporate radiation flux information during the optimization process in order to determine the optimal trajectories. Considering orbit-raising scenarios from the Low-Earth Orbit to the Geostationary Orbit (GEO), we present minimum fluence solutions and provide a comparison with the minimum time solutions.*

Keywords: *Low-thrust trajectory optimization, Electric Orbit-raising, Van Allen belt radiation*

1. Introduction

Traditionally, the space industry has relied upon chemical propulsion systems for supporting the primary propulsive activities of a satellite like orbit-raising to the Geostationary Earth orbit (GEO). High power requirements of electric propulsion (EP) devices and associated long orbit-raising time have limited their use for secondary propulsive activities that include in-orbit operations like station-keeping and attitude control. Hence, the mass savings provided by EP devices owing to their superior propellant management is not completely realized for current satellites that employ a hybrid chemical and electric propulsion systems. The ability of satellites to perform electric orbit-raising will potentially lead to significant mass savings that will allow additional payload capabilities for the existing satellite or the development of lighter satellites. Furthermore, ability of satellites to perform all propulsive tasks using EP devices can potentially reduce complexity of design compared to satellites with hybrid propulsion system. In recent times, there has been an increased interest among telecommunication satellite operators around the world in using all-electric propulsion in their future satellites [1, 2].

In this paper, we focus on the electric orbit-raising problem. One of the major concerns about electric orbit-raising is the damage caused by incident radiation during the long transit through the Van Allen belts surrounding the Earth. Electric orbit-raising, being a slow process due to the low thrust provided by electric engines, exposes the satellite to Van Allen radiation that causes considerable degradation of satellite solar arrays during the long transit [3, 4, 5]. This degradation not only reduces the power availability during the orbit-raising maneuver, but also reduces the Beginning-of-Lifetime (BOL) power of a satellite, thereby affecting all future operations of the satellite once it is deployed in its orbit. In the last couple of decades, many studies have captured the trade-offs among transfer time, mass savings and radiation exposure for a variety of mission scenarios [6,7,8,9,10]. However, all these studies have considered minimum time trajectories to the

GEO [7, 9, 11, 10, 12, 13, 14]. A minimum-time trajectory would correspond to minimum solar cell damage only if the intensity of the radiation is uniform throughout the Van Allen belt. Obviously, this is not the case because the radiation flux varies with altitude and latitude and a minimum-time trajectory will likely traverse the regions of higher radiation flux causing more damage to the solar arrays (and possibly other electronics too).

Our aim is to determine electric orbit-raising trajectories that minimize radiation fluence incurred by a satellite as it transfers from an arbitrary starting orbit to the Geostationary orbit (GEO). This will help to deliver the satellite to GEO with maximum BOL power for the solar arrays and will also limit the impact of radiation damage on other electronic components as well. So that avoidance of radiation damage does not come at the cost of unusually long transfer time, we impose an upper bound on the time of orbit-raising. In other words, we develop a new formulation for the orbit-raising problem that incorporates flux information for geomagnetically trapped radiation and determines the minimum fluence trajectories with constraint on the total time of transfer. In this paper, we describe this formulation and illustrate how the minimum fluence solutions differ from those minimizing time. Providing numerical examples for orbit-raising from the Low-Earth Orbit (LEO) to the GEO, we study the difference in the minimum-time and minimum-fluence solutions for planar and non-planar orbt-raising maneuvers. The impact of the time constraint on the amount of radiation exposure experienced by the satellite during the orbit-raising maneuver.

The primary contribution of this paper is to incorporate radiation flux information within an optimization framework in order to determine minimum radiation fluence solution to low-thrust orbit-raising problem. To this end, this paper is a first-step towards developing a generalized framework capable of minimizing an arbitrary mission objective that is a complex function of fuel expenditure, transfer time and radiation fluence. The paper is organized as follows: in section 2, we present the mathematical formulation for the time-constrained minimum radiation optimal control problem. The optimal control law, similar to the cases of minimum-time and minimum-fuel problems, is bang-bang in nature and the decision to thrust or coast is based on the sign of a switching function. We demonstrate that the case when the switching function is zero forces the thrust to be zero and hence no singular solution exists. We complete the mathematical formulation of the problem in section 3 by describing the satellite motion and the geomagnetic field using using spherical coordinates. In section 4, we present a direct optimization based methodology for computing low-thrust solutions that minimize radiation fluence. We use minimum time trajectories and a bang-bang thrusting scheme as initial guess for our developed solver. In section 5, we illustrate by numerical examples minimum fluence solutions as obtained using our methodology and provide a comparison with minimum time solutions.

2. Minimum Radiation Optimal Control Problem

In this section, we formulate the minimum radiation orbit-raising problem as an optimal control problem and derive the optimal control law from the Euler-Lagrange equations associated with the problem. More specifically, we show that the optimal control is bang-bang and also prove the non-existence of a singular case in which the thrust becomes indeterminate.

2.1. Mathematical Formulation

Let us denote by $\mathbf{r}(t)$ and $\mathbf{v}(t)$ the position and velocity of a satellite with respect to an inertial frame attached to the center of the Earth at any given time t. Also, let $m(t)$ denote the mass of the satellite as a function of time. At any time t, we denote the state of the satellite by $(\mathbf{r}(t), \mathbf{v}(t), m(t))$. Let us consider that the satellite moves from an initial state $(\mathbf{r}_0, \mathbf{v}_0, m_0)$ to a final state $(\mathbf{r}_f, \mathbf{v}_f, m_f)$ in time t_f. The initial state is known a priori. For the final state, only the position and velocity are known, that is, m_f and t_f are unknown. Note that we are considering a time constrained problem, that is, there is an upper bound on the final transfer time $t_{f,\max}$ within which the transfer must be completed. Now, let us denote by $T(t)$ and $\mathbf{u}(t)$ the magnitude and direction of the thrust of the propulsion system employed by the satellite. We represent by $\mathbf{g}(r)$ the gravitational acceleration experienced by the satellite at a location described by $\mathbf{r}$. Then, the equations of motion of the satellite can be written as:

$$\dot{\mathbf{r}} = \mathbf{v}, \tag{1}$$

$$\dot{\mathbf{v}} = \mathbf{g}(r) + \frac{T}{m}\mathbf{u}, \tag{2}$$

$$\dot{m} = -\frac{T}{c}, \tag{3}$$

where c is the specific impulse of the engine. Note that $\mathbf{u}$ is an unit vector and must satisfy $\mathbf{u}^T\mathbf{u} = 1$. Also, considering that there is a maximum thrust that can be provided by a given electric propulsion device, we have $0 \leq T \leq T_{\max}$.

The damage caused by the Van Allen belt radiation during the orbit-raising maneuver depends on the flux of particles in the regions of Van Allen belt traversed by the satellite, energy levels of the impacting particles and the material properties of the electronics absorbing the radiation dose. To minimize the damage or dose experienced by a solar array (or other relevant electronics) along an orbit-raising trajectory, one needs to minimize an integral of the form

$$\int_0^{t_f} \Psi_m(\Phi(\mathbf{r}), E)\, dt$$

that represents the total damage or dose experienced along the trajectory for a certain material m for solar array or other electronics (say, GaAs). For a particular material m, the dose is a function of the flux of all particles of energy level greater than E [15, 16]. In the current paper, we use a simplified form of the objective function by considering $\Psi_m(\Phi(\mathbf{r}), E) = \Phi(\mathbf{r})$ and minimize the total radiation fluence from all particles encountered by the satellite within the Van Allen belts. The motivation is to develop a mathematical framework (independent of any particular electronics) that can be extended in future to minimize the total material-specific damage or dose. In other words, we formulate the optimal control problem as:

$$\min J = \int_0^{t_f} \Phi(\mathbf{r})\, dt \tag{4}$$

subject to dynamic constraints given by Eq. 1-3, boundary conditions given by

$$\mathbf{r}(0) = \mathbf{r}_0,\ \mathbf{v}(0) = \mathbf{v}_0,\ m(0) = m_0, \mathbf{r}(t_f) = \mathbf{r}_f,\ \mathbf{v}(t_f) = \mathbf{v}_f, \tag{5}$$

constraints on the engine thrust given by

$$0 \leq T \leq T_{\max}, \ \mathbf{u}^T\mathbf{u} = 1, \tag{6}$$

and constraint on the time of transfer

$$t_f \leq t_{f,\max}. \tag{7}$$

2.2. Necessary Conditions of Optimality

The Hamiltonian for the system can be expressed as

$$H = \Phi(\mathbf{r}) + \boldsymbol{\lambda}_r^T\mathbf{v} + \boldsymbol{\lambda}_v^T\left(\mathbf{g}(r) + \frac{T}{m}\mathbf{u}\right) + \lambda_m\left(-\frac{T}{c}\right) + \eta\left(\mathbf{u}^T\mathbf{u} - 1\right), \tag{8}$$

where $\eta \geq 0$. The first order necessary conditions for optimality (Euler-Lagrange equations [17]) can then be written as

$$\dot{\boldsymbol{\lambda}}_r = -\left(\frac{\partial H}{\partial \mathbf{r}}\right)^T = -\frac{\partial \Phi}{\partial \mathbf{r}} - \frac{\partial \mathbf{g}(r)\,\mathbf{r}}{\partial r}, \tag{9}$$

$$\dot{\boldsymbol{\lambda}}_v = -\left(\frac{\partial H}{\partial \mathbf{v}}\right)^T = -\boldsymbol{\lambda}_r, \tag{10}$$

$$\dot{\lambda}_m = -\left(\frac{\partial H}{\partial m}\right) = \frac{T}{m^2}\boldsymbol{\lambda}_v^T\mathbf{u}, \tag{11}$$

$$0 = \left(\frac{\partial H}{\partial \mathbf{u}}\right) = \frac{T}{m}\boldsymbol{\lambda}_v + 2\eta\mathbf{u}. \tag{12}$$

Since terminal cost is zero for the problem in consideration and Hamiltonian is not an explicit function of time, we must have at any instant of time

$$H = 0. \tag{13}$$

2.3. Optimal Control Law

From Eq. 12, we have that

$$\mathbf{u} = -\frac{T}{2\eta m},$$

which along with $\mathbf{u}^T\mathbf{u} = 1$ yields

$$\mathbf{u} = -\frac{\boldsymbol{\lambda}_v}{\lambda_v}. \tag{14}$$

Hence, the thrust direction has to be directed opposite to the primer vector, a well-known result in spacecraft trajectory optimization [18]. Using the direction of thrust in the definition of Hamiltonian in Eq. 8, we have

$$H = \Phi(\mathbf{r}) + \boldsymbol{\lambda}_r^T\mathbf{v} + \boldsymbol{\lambda}_v^T\mathbf{g}(r) - \frac{T}{m}S, \tag{15}$$

where the switching function [19] is defined by

$$S = \lambda_v + \frac{m}{c}\lambda_m. \tag{16}$$

It can be easily seen that the Hamiltonian is minimized if

$$T = \begin{cases} T_{\max}, & \text{if } S > 0, \\ 0, & \text{if } S < 0, \\ 0 \le T \le T_{\max}, & \text{if } S = 0. \end{cases} \tag{17}$$

The case when the switching function is 0 poses a challenge as the thrust becomes indeterminate. We however show that if S is indeed 0 over a time interval, the thrust has to be zero at all times within that interval.

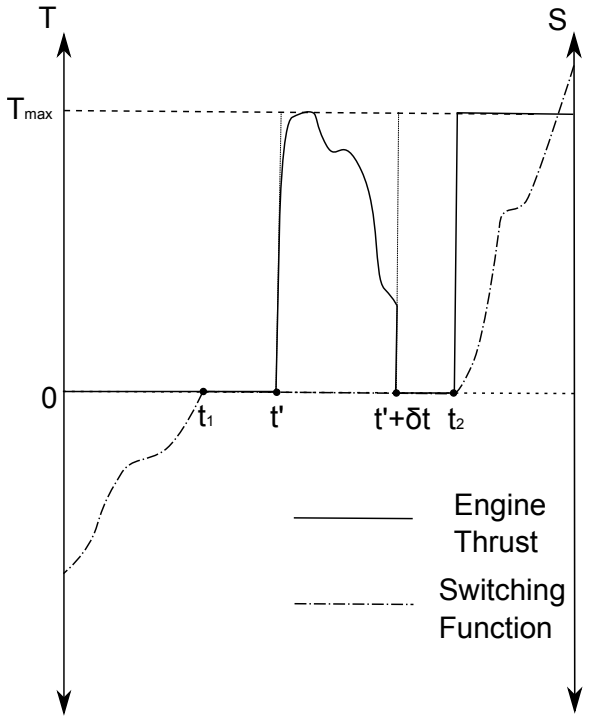

Figure 1. Variation of thrust T and switching function S with time (switching function S is zero for all $t_1 \le t \le t_2$).

2.4. Singular Solution: $S = 0$

Let us assume that over an interval of time $[t_1, t_2] \subseteq [0, t_f]$, the switching function $S = 0$ (see Fig. 1). This implies that

$$S = 0,\ \dot{S} = 0,\ \ddot{S} = 0 \ldots \tag{18}$$

Now, $S = 0$ implies

$$\lambda_v = -\frac{m}{c}\lambda_m. \tag{19}$$

Also, note that Eq. 11 and Eq. 14 imply

$$\dot{\lambda}_m = -\frac{T\lambda_v}{m^2}. \tag{20}$$

Using Eq. 3 and Eq. 20, we have

$$\dot{S} = \dot{\lambda}_v + \frac{\dot{m}}{c}\lambda_m + \frac{m}{c}\dot{\lambda}_m = \dot{\lambda}_v - \frac{T}{cm}S = \dot{\lambda}_v. \tag{21}$$

In other words, Eq. 18 implies

$$\dot{\lambda}_v = \ddot{\lambda}_v = \ldots = 0. \tag{22}$$

This means that the magnitude of the primer vector must be constant for all $t \in [t_1, t_2]$ whenever $S = 0$. In other words, we can say from Eq. 19 that

$$m\,\lambda_m = \text{ constant , for all } t \in [t_1, t_2]\,, \tag{23}$$

Let us now consider that $T > 0$ (strictly greater than 0) over a time interval $[t', t' + \delta t] \subseteq [t_1, t_2]$. We therefore must have from Eq. 23 the following relation

$$m\left(t'\right)\lambda_m\left(t'\right) = m\left(t' + \delta t'\right)\lambda_m\left(t' + \delta t'\right). \tag{24}$$

Now, note that mass of the satellite is a strictly monotonically decreasing function of time if $T > 0$ (Eq. 3). We therefore have

$$m\left(t'\right) > m\left(t' + \delta t'\right). \tag{25}$$

Considering Eq. 20, we have that $\dot{\lambda}_m$ is a strictly monotonically decreasing function of time (unless $\lambda_v = 0$) since $T > 0$ for all $t \in [t', t' + \delta t]$. However, using (25), we have from (24),

$$\lambda_m\left(t'\right) = \frac{m\left(t' + \delta t'\right)}{m\left(t'\right)}\lambda_m\left(t' + \delta t'\right) < \lambda_m\left(t' + \delta t'\right), \tag{26}$$

which contradicts the fact that λ_m is a strictly monotonically decreasing function in the time interval $[t', t' + \delta t]$. Hence, we have proved that we cannot have $T > 0$ if $S = 0$ and $\lambda_v \neq 0$. If $\lambda_v = 0$, then we have from Eq. 19 that $\lambda_m = 0$. Also, from Eq. 10, we have $\boldsymbol{\lambda}_r = \mathbf{0}$, so that the Hamiltonian becomes $H = \Phi(r)$ that is a function of Earth's magnetic field and cannot be zero (as required by Eq. 13). Hence, we cannot have $\lambda_v = 0$ and therefore must have $T = 0$ for all $t \in [t_1, t_2]$. In other words, we have $S = 0$ implies $T = 0$. We can therefore write the optimal control law as follows:

$$\boxed{T = \begin{cases} T_{\max}, & \text{if } S > 0, \\ 0, & \text{if } S \leq 0, \end{cases}} \tag{27}$$

3. Mathematical Formulation

In this section, we explicitly outline the various functions used in the previous section and complete the mathematical description of the minimum fluence low-thrust trajectory optimization problem. To this end, we describe the dynamics of the satellite and the Earth's magnetic field in the spherical reference frame and describe how we incorporate information about geomagnetically trapped radiation within the optimization framework.

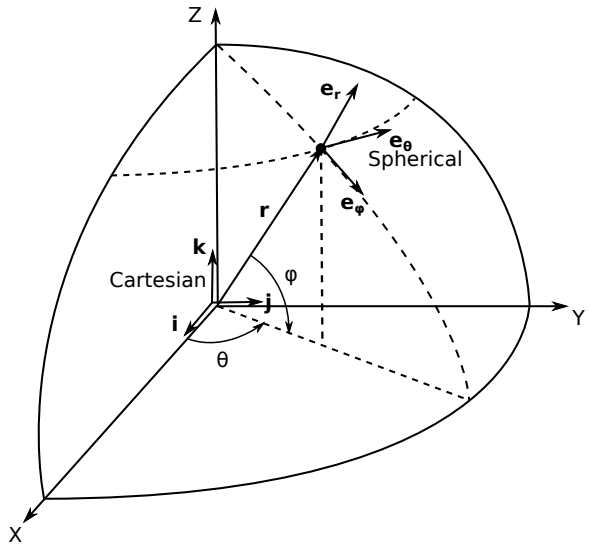

Figure 2. Spherical reference system for describing equations of motion of satellite.

3.1. Problem Description and Notations

Let us consider a satellite in an arbitrary initial orbit, which can be circular or elliptical and may have inclination with respect to Earth's equatorial plane. Let $\mathbf{x}(t)$ denote the state of the satellite at any time t. The state vector is comprised of the satellite's position vector $\mathbf{r}(t)$, the velocity vector $\mathbf{v}(t)$ and the mass $m(t)$. At $t = 0$, the satellite is at its initial orbit into which the satellite has been injected by an appropriate launcher. This initial orbit is henceforth referred to as an injection orbit. The initial state of the satellite $\mathbf{x}(0)$ is defined by the position and velocity of the satellite in the injection orbit and the initial mass $m(0)$. We consider that the satellite employs an electric propulsion system that provides a maximum thrust $T_{\max}$ and a specific impulse of I_{sp}. We assume that the satellite uses the electric engine to transfer from the injection orbit to the GEO (which is a circular orbit of altitude 35,786 km with zero inclination). The GEO therefore provides constraints for the position $\mathbf{r}(t_f)$ and velocity $\mathbf{v}(t_f)$ at final time. The terminal time t_f of the transfer is free, but has an upper bound $t_f^{\max}$ within which the orbit-raising maneuver has to be completed. We wish to minimize the radiation fluence experienced by the satellite during its transfer to GEO.

3.2. Equations of Motion

We use a spherical reference frame to describe the motion of the satellite. Figure 2 depicts this spherical reference frame and its orientation with respect to the Cartesian reference frame fixed to the Earth in terms of the azimuthal angle θ and the polar angle ϕ. Expressed in terms of the unit vectors $\mathbf{e}_r$, $\mathbf{e}_\theta$ and $\mathbf{e}_\phi$, the kinematics of the satellite is given by the velocity vector[20]

$$\mathbf{v} = r\dot{\phi}\mathbf{e}_\phi + r\dot{\theta}\sin\phi\,\mathbf{e}_\theta + \dot{r}\mathbf{e}_r, \tag{28}$$

and the acceleration vector[20]

$$\begin{aligned}\mathbf{a} &= \left(r\ddot{\phi} + 2\dot{r}\dot{\phi} - r\dot{\theta}^2\sin\phi\cos\phi\right)\mathbf{e}_\phi \\ &+ \left(r\sin\phi\,\ddot{\theta} + 2\dot{r}\dot{\theta}\sin\phi + 2r\dot{\phi}\,\dot{\theta}\sin\phi\right)\mathbf{e}_\theta + \left(\ddot{r} - r\dot{\theta}^2\sin^2\phi - r\dot{\phi}^2\right)\mathbf{e}_r.\end{aligned}$$

Let the thrust provided by the satellite engine be denoted by T and the angle the thrust vector makes with the plane defined by the unit vectors $\mathbf{e}_r$ and $\mathbf{e}_\theta$ be given by β. Also, let us denote by α the angle the projection of the thrust vector on the same plane makes with the unit vector $\mathbf{e}_r$. The control vector $\mathbf{u}$ representing the thrust of the electric engine employed by the satellite is therefore given by:

$$\mathbf{u} = T\sin\beta\mathbf{e}_\phi + T\cos\alpha\sin\beta\mathbf{e}_\theta + T\cos\alpha\cos\beta\mathbf{e}_r. \tag{29}$$

The equations of motion of the satellite can be written as follows:

$$\ddot{r} - r\dot{\theta}^2\sin^2\phi - r\dot{\phi}^2 = \frac{T}{m}\cos\alpha\cos\beta \tag{30a}$$

$$r\sin\phi\,\ddot{\theta} + 2\dot{r}\dot{\theta}\sin\phi + 2r\dot{\phi}\dot{\theta}\sin\phi = \frac{T}{m}\sin\alpha\cos\beta \tag{30b}$$

$$r\ddot{\phi} + 2\dot{r}\dot{\phi} - r\dot{\theta}^2\sin\phi\cos\phi = \frac{T}{m}\sin\beta \tag{30c}$$

Let us denote by u, v and w the components of velocity along the unit vectors $\mathbf{e}_r$, $\mathbf{e}_\theta$ and $\mathbf{e}_\phi$. Also, let us now denote the state vector of the satellite by $\mathbf{x}(t) \equiv (r(t), \theta(t), \phi(t), u(t), v(t), w(t), m(t))$. The equations of motion can be written in the following state-space form:

$$\dot{r} = u, \tag{31a}$$

$$\dot{\theta} = \frac{v}{r\sin\phi}, \tag{31b}$$

$$\dot{\phi} = \frac{w}{r}, \tag{31c}$$

$$\dot{u} = -\frac{\mu}{r^2} + \frac{v^2+w^2}{r} + \frac{T}{m}\cos\alpha\cos\beta \tag{31d}$$

$$\dot{v} = -\frac{uv + vw\cot\phi}{r} + \frac{T}{m}\sin\alpha\cos\beta \tag{31e}$$

$$\dot{w} = \frac{-uw + v^2\cot\phi}{r} + \frac{T}{m}\sin\alpha \tag{31f}$$

$$\dot{m} = -\frac{T}{c} \tag{31g}$$

3.3. Geomagnetically Trapped Radiation

Let us consider the magnetic field (or flux density) of the Earth to be represented by the field of a magnetic dipole centered with the Earth and with an axis parallel to the Earth's spin axis that passes through its center of mass. In spherical coordinates, the magnetic field can be written as[21]:

$$\mathbf{B} = B_r\mathbf{e}_r + B_\phi e_\phi + B_\theta e_\theta, \tag{32}$$

where the three components can be written as

$$B_r = -\frac{2B_0}{(r/R)^3} cos\phi,\ B_\phi = -\frac{B_0}{(r/R)^3} sin\phi,\ B_\theta = 0, \tag{33}$$

where m is the magnetic dipole moment of Earth, R is the radius of the Earth, θ is the longitude, ϕ is the colatitude and B_0 is the equatorial value of geomagnetic flux density

$$B_0 = \frac{\mu_0 m}{4\pi R^3}. \tag{34}$$

The magnitude of the geomagnetic field for a spin axis aligned dipole can be written as

$$B = \frac{B_0 m}{(r/R)^3} \left(1 + 3cos^2\phi\right)^{1/2}. \tag{35}$$

In terms of a local vertical reference frame, the magnetic field vector has an angle of declination D and an angle of inclination I. The declination of the field line is given by

$$\tan D = -\frac{B_\theta}{B_\phi}, \tag{36}$$

which is 0 for the spin axis aligned dipole. The inclination of the field line is given by

$$\tan I = -\frac{B_r}{B_\phi} = -2\cot\phi. \tag{37}$$

The geometry of the field line can be expressed as

$$\tan I = -\frac{dr}{rd\phi}. \tag{38}$$

Substituting equation(37) and integrating, we obtain from equation(39) the following equation for the magnetic field lines:

$$r = LR\sin^2\phi \tag{39}$$

in terms of parameter L which is the distance to the field line at $\phi = \pi/2$, that is, at the equator. Substituting equation(39) in (35), we have the relationship between B and L:

$$B = \frac{B_0}{(r/R)^3} \left(4 - \frac{3r}{LR}\right)^{1/2}. \tag{40}$$

McIlwain's (B,L) coordinate system [22] is used to conveniently compute properties of the trapped charged particles because it is a means of converting the three-dimensional space into a two-dimensional space based on the fact that the dipole field is axially symmetric.

Charged particles, primarily electrons and protons, are trapped in the Earth's magnetosphere originate from solar wind and the decay of neutrons produced by the interactions of galactic cosmic rays with the Earth's atmosphere. Typical models of the trapped radiation for the Earth are the AP model for protons and AE model for electrons developed by NASA [23]. The model gives trapped omnidirectional proton and electron fluxes (particles per unit area per unit time) of energies between 0.1 and 400 MeV between L-shell values of 1.15 and 6.5 as a function of geomagnetic coordinates B and L. At any point on the satellite trajectory, we compute the geomagnetic coordinates and use a look-up table with AP8 and AE8 models to obtain the proton and electron flux. The total radiation fluence is the radiation flux integrated over time as given by Eq. 4.

4. Solution Methodology

In this section, we discuss the methodology we follow for solving the optimal control problem. We follow a direct optimization approach which is known to be more robust numerically in terms of initial guesses and solution convergence [24]. We extend our developed solver in reference [14] by incorporating radiation model within the optimization framework.

4.1. Direct Transcription and Collocation

In order to solve the optimization problem for each scenario, we use a direct optimization scheme. The scheme converts the trajectory optimization problem to a parameter optimization problem using direct transcription and collocation, and then uses a Non-Linear Programming (NLP) problem solver (IPOPT [25], LOQO [26]) to determine the solution. The time variable is discretized using a non-dimensional time-like variable τ and final time t_f is also a parameter in the problem:

$$0 = \tau_1 < \tau_2 < \ldots < \tau_n = 1, \;\; t_k = t_f \tau_k. \tag{41}$$

The state $\mathbf{x}$ and control $\mathbf{u}$ variables of a continuous trajectory are also discretized based on the selected time-grid:

$$\mathbf{x}_k = \mathbf{x}(t_k), \, \mathbf{u}_k = \mathbf{u}(t_k). \tag{42}$$

Using a trapezoidal discretization scheme, we can approximate the dynamic constraints as follows:

$$\boldsymbol{\zeta}_k = \mathbf{x}_{k+1} - \mathbf{x}_k - \frac{h_k}{2} \left[\mathbf{f}\left(\mathbf{x}_{k+1}, \mathbf{u}_{k+1}\right) + \mathbf{f}\left(\mathbf{x}_k, \mathbf{u}_k\right) \right]. \tag{43}$$

Note that we have a set of defects corresponding to each of the equations of motion given in (31), that is, $\boldsymbol{\zeta}_k \equiv \left(\boldsymbol{\zeta}^r, \boldsymbol{\zeta}^\theta, \boldsymbol{\zeta}^\phi, \boldsymbol{\zeta}^u, \boldsymbol{\zeta}^v, \boldsymbol{\zeta}^w \right)$, where the superscript indicates the equation of motion that the defect corresponds to. If these defects are driven to zero, then the dynamic constraints (equations of motion) will hold approximately at each of the segments created by the discretization process. The set $\left(\mathbf{x}_1, \mathbf{x}_2, \ldots, \mathbf{x}_n; \mathbf{u}_1, \mathbf{u}_2, \ldots, \mathbf{u}_n; t_f \right)$ represents the decision variables of the resulting parameter optimization problem. During the optimization process (using a NLP solver), the defects are driven to zero. Using the discretization scheme, we can also write down the objective function (radiation fluence) as:

$$c = \sum_{k=1}^{n-1} \frac{1}{2} \left(\Phi\left(r_k, \theta_k, \phi_k\right) + \Phi\left(r_{k+1}, \theta_{k+1}, \phi_{k+1}\right) \right) \left(t_{k+1} - t_k \right) \tag{44}$$

Instead of using a trapezoidal discretization, we may use a more accurate (but computationally more complex) Hermite-Simpson trapezoidal discretization to approximate the dynamic constraints. To this end, we additionally consider the mid-point of the segments $\mathbf{u}_m$ and set up the defects as:

$$\boldsymbol{\zeta}_k = \mathbf{x}_{k+1} - \mathbf{x}_k - \frac{h_k}{6} \left[\mathbf{f}\left(\mathbf{x}_{k+1}, \mathbf{u}_{k+1}\right) + 4\mathbf{f}\left(\mathbf{x}_{mk}, \mathbf{u}_{mk}\right) + \mathbf{f}\left(\mathbf{x}_k, \mathbf{u}_k\right) \right], \tag{45}$$

where the values of the state variables at the mid-point of segments are given by

$$\mathbf{x}_{mk} = \frac{1}{2} \left[\mathbf{x}_{k+1} + \mathbf{x}_k \right] + \frac{h_k}{8} \left[\mathbf{f}\left(\mathbf{x}_k, \mathbf{u}_k\right) - \mathbf{f}\left(\mathbf{x}_{k+1}, \mathbf{u}_{k+1}\right) \right]. \tag{46}$$

When we use the Hermite-Simpson discretization scheme, the control variables evaluated at the mid-point of the segments also become a part of the decision variables:

$$\left(\mathbf{x}_1, \mathbf{x}_2, \ldots, \mathbf{x}_n; \mathbf{u}_1, \mathbf{u}_2, \ldots, \mathbf{u}_n; \mathbf{u}_{m1}, \mathbf{u}_{m2}, \ldots, \mathbf{u}_{mn}; t_f\right).$$

4.2. NLP Solvers

We have set up two independent methods of solving the NLP associated with the parametric optimization problem. First, we set up the NLP using Matlab and use the solver IPOPT * (acronym for "Interior Point Optimizer") to obtain the optimal trajectory. Second, we set up the model of the optimization problem in AMPL [28] (acronym for "A Mathematical Programming Language") and use LOQO to solve the problem. Both NLP solvers IPOPT and LOQO are interior-point based methods and are therefore suitable for large-scale non-linear optimization. Also, both IPOPT and LOQO can take advantage of the sparsity of the Jacobian and Hessian matrices to efficiently solve the problem. For the Matlab-IPOPT interface we provide analytic expressions for the first-order and second-order derivatives for the associated NLP; for the AMPL-LOQO interface, these are computed numerically by the solvers. The lack of guarantees of the global optimality of a generated solution of the NLP justifies the use of two numerical methods to compute solutions for the same problem. Considering a Hermite-Simpson discretization, the first-order derivative information includes the gradient of the objective function

$$\nabla c \equiv \left(\frac{\partial c}{\partial \mathbf{x}_k}, \frac{\partial c}{\partial \mathbf{u}_k}, \frac{\partial c}{\partial \mathbf{u}_{mk}}, \frac{\partial c}{\partial t_f}\right). \tag{47}$$

and the Jacobian of the constraints:

$$\nabla \zeta_k \equiv \left(\frac{\partial \zeta_k}{\partial \mathbf{x}_k}, \frac{\partial \zeta_k}{\partial \mathbf{u}_k}, \frac{\partial \zeta_k}{\partial \mathbf{u}_{mk}}, \frac{\partial \zeta_k}{\partial t_f}\right). \tag{48}$$

The second-order derivative information includes computation of the Hessian matrix:

$$H \equiv \sigma_f \nabla^2 c + \sum_k \lambda_k \nabla^2 \zeta_k, \tag{49}$$

which usually is a sparse matrix. For a trapezoidal discretization scheme, for which control variables at the mid-points of the segments are not present in the formulation, we use the same equations without the terms for $\mathbf{u}_{mk}$.

We illustrate the computation of Jacobian and Hessian with an example by considering the defect corresponding to the first equation of motion (30a) evaluated at node k. Using (45) for the trapezoidal discretization, the defect can be written as:

$$\zeta_k^r = r_{k+1} - r_k - \frac{h_k}{2}\left(u_k + u_{k+1}\right).$$

*IPOPT requires a sparse symmetric linear solver for its operation, we use the Harwell Subroutine Library (HSL) functions [27] MA27 and MC19 for the purpose.

The non-zero partial derivatives for this defect can then be written as:

$$\frac{\partial \zeta_k^r}{\partial r_k} = -1,\ \frac{\partial \zeta_k^r}{\partial r_{k+1}} = 1,\ \frac{\partial \zeta_k^r}{\partial u_k} = -\frac{h_k}{2},\ \frac{\partial \zeta_k^r}{\partial u_{k+1}} = -\frac{h_k}{2},\ \frac{\partial \zeta_k^r}{\partial t_f} = -\frac{\Delta\tau}{2}\left(u_k + u_{k+1}\right),$$

where $\Delta\tau$ equals the difference between the values of the time-like variable τ at nodes k and $k+1$. Note that for an uniform distribution of nodes, $\Delta\tau = 1/n$. Also, note that partial derivatives of ζ_k^r with respect to all other decision variables is zero. The second-order partial derivatives can be determined directly from the first-order derivatives. For the present case, the non-zero second-order derivatives are given by:

$$\frac{\partial^2 \zeta_k^r}{\partial t_f \partial u_k} = -\frac{\Delta\tau}{2},\ \frac{\partial^2 \zeta_k^r}{\partial t_f \partial u_{k+1}} = -\frac{\Delta\tau}{2}.$$

As before, remaining second-order derivatives are zero for the defect ζ_k^r. Similarly, all of the first-order and second-order derivatives are computed for the remaining set of defects given by $\zeta^\theta, \zeta^\phi, \zeta^u, \zeta^v, \zeta^w$. Note that in the absence of analytic expressions for the radiation fluence terms, $\nabla^2 c$ is evaluated numerically. The evaluation of the first-order derivatives completes the computation of the Jacobian, while the evaluation of the second-order derivatives completes the Hessian computation. The parameters σ_f and λ_k are internally generated by IPOPT during the course of executing the NLP.

5. Numerical Examples

In this section, we present solutions obtained using our methodology for low-thrust orbit-raising from LEO to the GEO. We also compare the obtained solutions with the minimum-time solutions for both planar and non-planar orbit-raising maneuvers. The minimum time solutions are derived using the tool developed in Ref. [14].

To this end, let us first consider the orbit-raising problem for transferring a satellite from an equatorial circular LEO orbit of radius 500 km to the GEO. Using a range of values for the engine thrust (0.3 N to 10 N) in order to cover a variety of thrusters from the BPT-4000 to the MPD thrusters, we compute the minimum-time solutions and use our developed model to compute the radiation fluence experienced by the satellite during the orbit-raising maneuver. The variation of radiation fluence is depicted in Fig. 3. When restricted to motion within a plane, the satellite spirals through similar radiation intensities while performing the orbit-raising maneuver and the radiation fluence is directly correlated with the time that the satellite spends within the Van Allen belts. Since thrusters offering lower thrust would mean a slower orbit-raising maneuver, the radiation fluence experienced by the satellite increases as the engine thrust decreases. Hence, it is fairly straightforward to see that the radiation effects would be the most pronounced for Hall and Ion thrusters, in fact several times compared to say a MPD thruster.

Let us now consider an example of a three-dimensional transfer in order to illustrate the impact of radiation as the satellite performs plane changes. We consider different inclinations of the initial injection orbit of the satellite and compute minimum-time solutions from the injection orbit to the GEO. We then compute the radiation fluence experienced by the satellite during the transfer. Figure 4 depicts the variation of the radiation fluence experienced by the satellite with the change

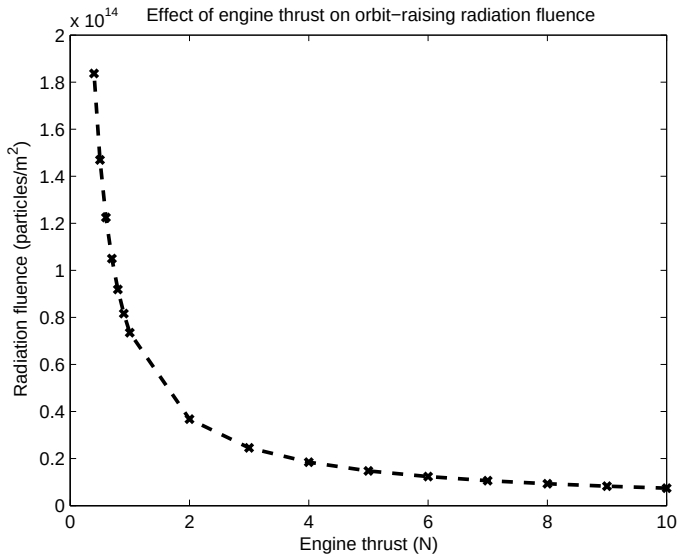

Figure 3. Radiation fluence experienced by satellites during planar minimum-time orbit-raising.

in inclination of the injection orbit. As the inclination changes from 0 degree, the transfer time

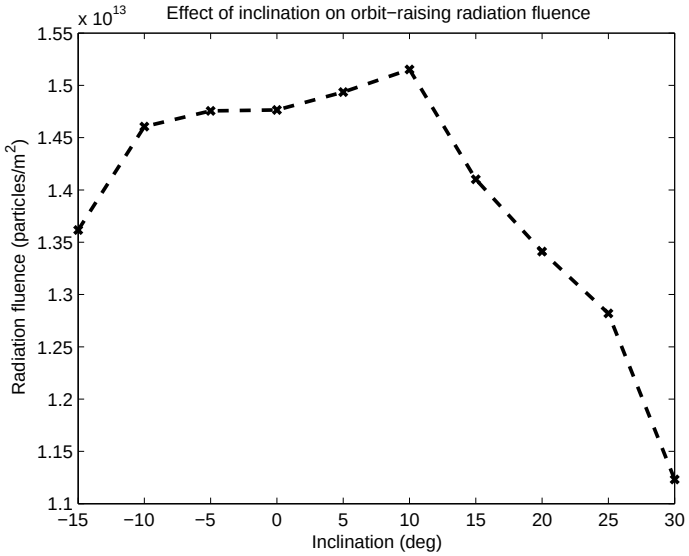

Figure 4. Radiation fluence experienced by satellites during minimum-time orbit-raising from inclined LEO injection orbit to the GEO.

increases, but the satellite traverses regions of reduced intensities of the Van Allen belts. The total radiation fluence captures the effect of both the competing factors of transfer time and the radiaiton flux. Figure 4 shows that the net effect of the two factors decreases the radiation fluence if we launch a satellite from a higher inclination orbit. One interesting point to note in this variation is that radiation fluence attains a maximum away from 0 degree because of the tilt in the Earth's magnetic axis with respect to its rotational axis.

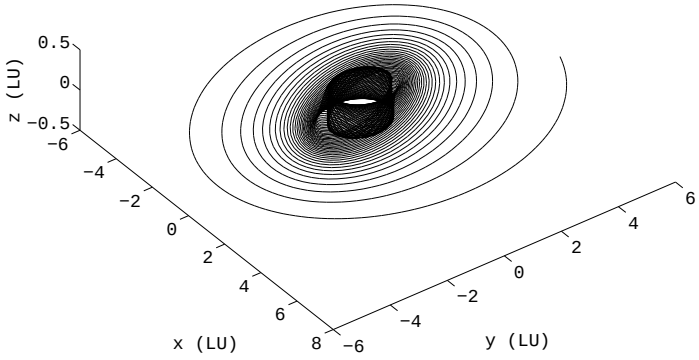

Figure 5. LEO-GEO minimum radiation fluence trajectory.

Let us now consider trajectories that incur minimum radiation fluence experienced by a satellite during orbit-raising maneuver. For the case when the satellite starts from an equatorial LEO orbit, we allow the solution to be non-planar and trade off time to traverse regions of lower radiation flux. However, the optimal solution determined by the solver is essentially the minimum-time solution. Performing plane changes may reduce the radiation flux experienced by the satellite; however, it also increases the transfer time and trading off time does not prove to be beneficial for the planar injection orbit case. The minimum radiation fluence can however be different from the minimum time solution for an inclined injection orbit case, as we demonstrate with the following example.

Let the satellite initiates a transfer from a LEO circular orbit that is inclined at an angle on 15 degrees to the equatorial plane. We also consider that the satellite employs an electric thruster with thrust 5 N and specific impulse of 2000 sec. We non-dimensionalize the different variables as follows: 1 LU represents the radius of the initial orbit, initial mass is considered to be 1 MU, μ is 1 so that the orbital velocity in the injection orbit is 1 and the time period is 2π units. We provide the minimum-time solution as an initial guess to our developed solver. Solving the minimum radiation problem with this initial guess yields a trajectory that incurs 3.9% less radiation fluence than the minimum-time trajectory, at the cost of a 10% increase in the transfer time. The optimal trajectory is depicted in Fig. 5 and the variation of the different states of the satellite corresponding to the optimal trajectory is depicted in Fig. 6.

6. Conclusions

In this paper, we develop a formulation to determine the minimum radiation fluence incurred by a satellite during electric orbit-raising to the Geostationary orbit. The optimal thrusting scheme for this problem is a bang-bang control and we prove the non-existence of a singular solution for such a problem. We use the bang-bang control scheme as a guess for the control variables in the direct optimization solver that incorporates radiation flux information (based on NASA AP8 and AE8 models). We provide the minimum time solutions as initial guesses to our solver. We consider

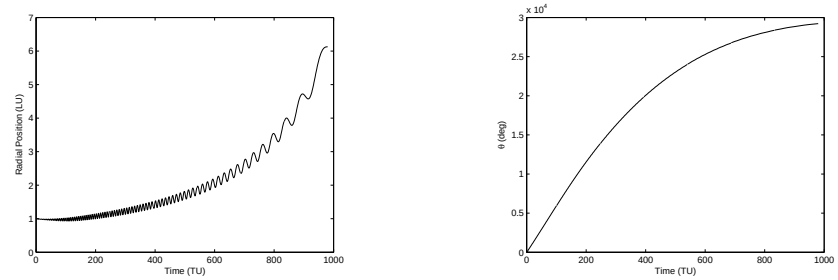

(a) r vs. t

(b) θ vs. t

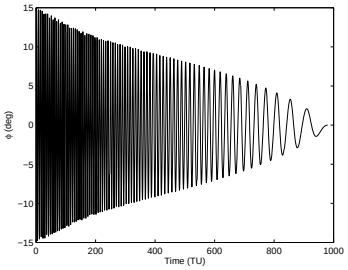

(c) ϕ vs. t

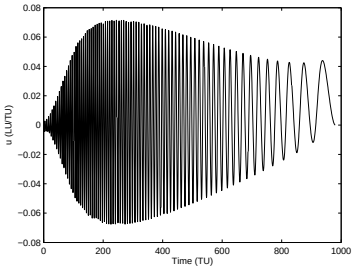

(d) u vs. t

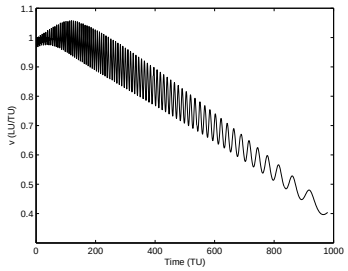

(e) v vs. t

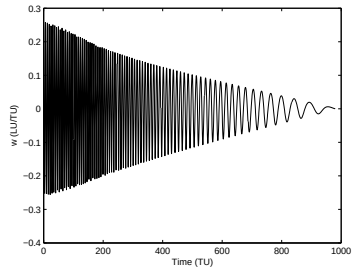

(f) w vs. t

Figure 6. Minimum radiation fluence solution.

planar and non-planar orbit-raising examples from LEO to GEO. When the satellite starts from an equatorial LEO orbit, we find that optimizing radiation fluence is the same as optimizing time. However, when the satellite starts from an inclined LEO orbit, the minimum radiation solution differs from the minimum time solution. In the future, we would use the developed tool to analyze a variety of orbit-raising scenarios, inclusion of eclipse constraints and energy storage options within the optimization framework in order to determine the trade-offs among mass, time and radiation fluence during electric orbit-raising. Future work will also consider the extension of the tool to determine trajectories to minimize material-specific radiation dose during electric orbit-raising.

7. Acknowledgement

This work was performed under grant number AGMT dated 4/1/2011 from SES Engineering. We thank Philippe Francken, Stan Russo, and Matthew Cooper of SES for their help and suggestions.

We also like to thank Mike Howard, senior-year undergraduate student at the Department of Me-

chanical and Aerospace Engineering, Princeton University, for writing the Matlab code to compute the radiation flux corresponding to a given location (r, θ, ϕ) of the satellite.

8. References

[1] SpaceNewsStaff. "SES Technology Chief Sings Praises of SpaceXs Falcon 9 Rocket.", June 2011.

[2] de Selding, P. B. "ABS, Satmex Banding Together for Boeing Satellite Buy.", March 2012.

[3] Smits, F. "The Degradation of Solar Cells under Van Allen Radiation." IEEE Transactions on Nuclear Science, Vol. 10, No. 1, pp. 88–96, 1963.

[4] Flanagan, P. F., Horsewood, J. L., and Pines, S. "Precision Orbit Raising Trajectories." "AIAA 11th Electric Propulsion Conference," New Orleans, LA, Mar 19-21 1975.

[5] Dailey, C. and Lovberg, R. "Shuttle to GEO Propulsion Trade Offs." "18th Joint Propulsion Conference," Cleveland, OH, Jun 21-23 1982.

[6] Redding, D. "Avoiding the Van Allen Belt in Low Thrust Transfer To Geosynchronous Orbit." "AIAA 21st Aerospace Sciences Meeting," Reno, NV, Jan 10-13 1983.

[7] Ennix, K. A., Dickey, M. R., Klucz, R. S., and Matuszak, L. W. "Electric vehicle Analyszer." "21st International Electric Propulsion Conference," Orlando, FL, July 18-20 1990.

[8] Free, B. "High Altitude Orbit Raising with On-Board Electric Power." "International Electric Propulsion Conference," Seattle, WA, Sep 1993.

[9] Fitzgerald, A. "The Effect of Solar Array Degradation in Orbit-Raising with Electric Propulsion." "International Electric Propulsion Conference," Seattle, WA, Sep 1993.

[10] Biagioni, L. "Evolutionary Optimization of Launch Vehicle Electric Propulsion Integration for GEO Missions." "Joint Propulsion Conference," Huntsville, AL, July 2000.

[11] Oleson, S. R. and Myers, R. M. "Launch vehicle and power level impacts on electric GEO insertion." "Joint Propulsion Conference and Exhibit," Buena Vista, FL, July 1-3 1996.

[12] Byers, D. C. and Dankanich, J. W. "Geosynchronous-Earth-Orbit Communication Satellite Deliveries with Integrated Electric Propulsion." Journal of Propulsion and Power, Vol. 24, No. 6, pp. 1369–1375, Nov-Dec 2008.

[13] Duchemin, O. B., Caratge, A., Cornu, N., Sannino, J.-M., Lassoudire, F., and Lorand, A. "Ariane 5-ME and Electric Propulsion: GEO Insertion Options." "47th Joint Propulsion Conference and Exhibit," 2011.

[14] Dutta, A., Libraro, P., Kasdin, N. J., and Choueiri, E. "A Direct Optimization Based Tool to Determine Orbit-Raising Trajectories to GEO for All-Electric Telecommunication Satellites." "AAS Astronautical Specialist Conference," Minneapolis, MN, Aug 2012. (submitted).

[15] Tada, H. Y. and Carter, J. R. "Solar Cell Radiation Handbook." JPL Publication 77-56, NASA, November 1977.

[16] AIAA, Reston, VA. Guide to Modeling Earth's Trapped Radiation Environment, 1999. AIAA G-083-1999.

[17] Bryson, A. and Ho, Y. Applied Optimal Control: Optimization Estimation and Control. Hemisphere Publishing Corporation, 1993.

[18] Lawden, D. Optimal Trajectories for Space Navigation. Butterworths, London, 1963.

[19] Russell, R. "Primer Vector Theory Applied to Global Low-Thrust Trade Space Studies." Journal of Guidance, Control and Dynamics, Vol. 30, No. 2, pp. 460–472, 2007.

[20] Kasdin, N. J. and Paley, D. A. Engineering Dynamics: A Comprehensive Introduction. Princeton University Press, Princeton, USA and Oxford, United Kingdom, 2011.

[21] Pisacane, V. L. The Space Environment and Its Effects on Space Systems. Education Series. American Institute of Aeronautics and Astronautics, Inc., Reston, VA, 2008.

[22] McIlwain, C. E. "Coordinates for Mapping the Distribution of Magnetically Charged Particles." Journal of Geophysical Research, Vol. 66, No. 11, pp. 3681–3691, November 1961.

[23] Jordan, C. E. "NASA Radiation Belt Models AP-8 and AE-8." Scientific Report No. 1 GL-TR-89-0267, Radex, Inc., Bedford, MA, September 1989.

[24] Conway, B. A., editor. Spacecraft Trajectory Optimization: Conway, Techniques and Technology. Cambridge University Press, 2010.

[25] Wchter, A. and Biegler, L. T. "On the implementation of an interior-point filter line-search algorithm for large-scale nonlinear programming." Mathematical Programming, Vol. 106, No. 1, pp. 25–57, 2006.

[26] Vanderbei, R. J. "LOQO: An Interior Point Code for Quadratic Programming." Optimization Methods and Software, Vol. 11, No. 1-4, pp. 451–484, 1999.

[27] Harwell Subroutine Library archives. A collection of Fortran codes for large scale scientific computation, 2011. Http://www.hsl.rl.ac.uk.

[28] Fourer, R., Gay, D., and Kernighan, B. AMPL: A Modeling Language for Mathematical Programming. Brooks/Cole Publishing Company, 2003.